JOURNAL OF GUIDANCE, CONTROL, AND DYNAMICS
Vol. 16, No. 1, January-February 1993

Digital Simulation of Atmospheric Turbulence for Dryden and von Kármán Models

T. R. Beal*
E-Systems, Inc., Greenville, Texas 75403

Algorithms are presented for generating discrete sample time histories of random atmospheric turbulence having statistical characteristics as prescribed by the Dryden and von Kármán models defined in MIL-F-8785C. When these algorithms are incorporated into a dynamic simulation, response of an aircraft to the turbulence can be predicted. Such information is useful both in the design stage and during the development phase of the aircraft. The von Kármán model is generated using a variation of the sum-of-sinusoids method, modified to reduce computation time. Techniques for improving computational speed are considered, and results of test runs are presented. The Dryden model is generated by passing band-limited white noise through appropriate linear filters. The input variance required to produce the desired output variance is determined as a function of the sample frequency. Generation of roll gust velocities is also addressed, as well as the application of lateral and vertical velocities to the computation of yaw and pitch moments on an aircraft.

Introduction

THE simulation of atmospheric turbulence is of considerable importance in the evaluation of aircraft performance. When used in conjunction with six-degree-of-freedom dynamic simulations, it gives the designer vital information about the expected behavior of the aircraft under various levels of turbulence. This information is useful for predicting structural loads and aircraft handling qualities. It can also be used to evaluate stability of onboard sensing equipment, as in aircraft used for surveillance missions. Integration of the simulated turbulence into real-time mechanical simulators provides a realistic basis for pilot flight training. The turbulence magnitudes are combined with simulated flight speed, appropriate aerodynamic derivatives, and aircraft configuration data to compute the magnitudes of actuator commands required to perturb the cockpit module in a manner typical of real life. Another application of vital importance is the prediction of aircraft performance for carrier landings, where one of the most significant factors is the effect of turbulence on the perturbations from an expected approach path. The turbulence spectra for the carrier application are somewhat different than the models considered in this paper; however, the techniques discussed herein are directly applicable to the carrier scenario.

The turbulence models frequently used to evaluate aircraft performance are the Dryden and von Kármán models. The power spectra for these models are defined analytically in MIL-F-8785C.[1] Each model consists of three velocity spectra, corresponding to the three axes associated with a body-fixed coordinate system. The frequency variable is spatially referenced to a "frozen" turbulence field, a concept that has been shown to produce realistic results for normal aircraft speeds. The advantage of the spatially referenced spectra is that the turbulence characteristics are independent of the aircraft speed. However, for the typical dynamic simulation, it is usually desirable to generate the turbulence velocities as functions of time. Using the transformations ω (rad/s) = Ω (rad/ft) · V (ft/s) and $\phi_{u,v,w}(\omega) = \Phi_{u,v,w}(\Omega)/V$, one could generate the turbulence velocities directly in the time domain, using methods analogous to those in this paper. A better approach, however, might be to retain the spatially referenced frequencies and spectra and use the space variable $x = Vt$ as an independent variable to generate the velocities.

The von Kármán form of the power spectral densities for the turbulence velocities is as follows:

$$\Phi_u(\Omega) = \sigma_u^2 \frac{2L_u}{\pi} \frac{1}{[1 + (1.339L_u\Omega)^2]^{5/6}} \tag{1}$$

$$\Phi_v(\Omega) = \sigma_v^2 \frac{L_v}{\pi} \frac{1 + (8/3)(1.339L_v\Omega)^2}{[1 + (1.339L_v\Omega)^2]^{11/6}} \tag{2}$$

$$\Phi_w(\Omega) = \sigma_w^2 \frac{L_w}{\pi} \frac{1 + (8/3)(1.339L_w\Omega)^2}{[1 + (1.339L_w\Omega)^2]^{11/6}} \tag{3}$$

The Dryden form of the power spectral densities for the turbulence velocities is as follows:

$$\Phi_u(\Omega) = \sigma_u^2 \frac{2L_u}{\pi} \frac{1}{1 + (L_u\Omega)^2} \tag{4}$$

$$\Phi_v(\Omega) = \sigma_v^2 \frac{L_v}{\pi} \frac{1 + 3(L_v\Omega)^2}{[1 + (L_v\Omega)^2]^2} \tag{5}$$

$$\Phi_w(\Omega) = \sigma_w^2 \frac{L_w}{\pi} \frac{1 + 3(L_w\Omega)^2}{[1 + (L_w\Omega)^2]^2} \tag{6}$$

where

u, v, w = velocities along x, y, z axes of aircraft, ft/s
Φ_u, Φ_v, Φ_w = power spectral densities of u, v, and w, ft^3/s^2
$\sigma_u, \sigma_v, \sigma_w$ = standard deviations of u, v, and w, ft/s
L_u, L_v, L_w = scale lengths for power spectra, ft

It can be verified by direct integration of each of the preceding spectral densities that

$$\sigma_{u,v,w}^2 = \int_0^\infty \Phi_{u,v,w}(\Omega)\, d\Omega$$

It will be assumed in this paper that the altitudes to be simulated are above 2000 ft, where the usual assumption is that $\sigma_u = \sigma_v = \sigma_w$ and $L_u = L_v = L_w$. The magnitudes of the standard deviations depend on the level of turbulence to be simulated and are selected accordingly. Reference 1 identifies these standard deviations in terms of exceedance probability at var-

Received July 8 1991; revision received Nov. 3, 1991; accepted for publication Feb. 1, 1992.

*Senior Staff Engineer, Greenville Division. Member AIAA.

ious altitudes. The same reference also specifies the following values of the scale lengths.
Von Kármán form:

$$L_u = L_v = L_w = 2500 \text{ ft}$$

Dryden form:

$$L_u = L_v = L_w = 1750 \text{ ft}$$

It has been recommended that the von Kármán model be used when feasible.[1] However, in practice the Dryden model is used much more frequently, mainly because of its simpler form and the ease with which it can be produced by passing white noise through linear filters. In this paper, techniques are presented for generating turbulence based on either the von Kármán or the Dryden model.

Von Kármán Turbulence

The technique presented herein for generating turbulence based on the von Kármán spectra is especially useful because of its applicability to any random process in which the spectral density is defined, either analytically or empirically. The method of generating the random function consists of summing an adequate number of sine functions with selected frequencies and random initial phases. It is appropriately called the sum-of-sinusoids method. The frequency of each sine function corresponds to the centroidal frequency of a segment of the known spectral density function, and the amplitude is such that the variance of the sine function is equal to the area under the curve between the bounding frequencies of the segment. Such a technique for modeling ship motions was first presented in the classic paper of St. Denis and Pierson[2] and is widely used and accepted today in simulating random ship motion. It has been used successfully in simulating the effects of various sea states on ship motion[3-5] and has been applied by this author in dynamic simulations to evaluate feasibility of shipboard recovery of an unmanned aircraft in extreme sea states.[6] Contributions of this paper include the judicious selection of the spectral density segments and the exploration of techniques for improving computational efficiency. The investigations are focused specifically on the von Kármán atmospheric model; however, the techniques can be applied to any random process.

The von Kármán spectra Φ_u and Φ_w are shown over a limited frequency range in Fig. 1, assuming unity values of σ_u and σ_w and scale lengths $L_u = L_w = 2500$ ft. The function Φ_v is identical to Φ_w and is omitted for simplicity. The methods presented for generating random time functions of w are applicable to the generation of v functions as well. The general forms for the random functions u and w are as follows:

$$u(x) = \sum (A_u)_i \sin[(\Omega_u)_i x + (\epsilon_u)_i] \tag{7}$$

$$w(x) = \sum (A_w)_i \sin[(\Omega_w)_i x + (\epsilon_w)_i] \tag{8}$$

where $(A_u)_i$ and $(A_w)_i$ are amplitudes (with dimensions ft/s) of the ith sine function of the u and w functions, respectively, and the summations extend over the number of segments of the spectral densities. Note that time functions $u(t)$ and $w(t)$ are obtained as follows: $u(t = x/V) = u(x)$ and $w(t = x/V) = w(x)$. The initial phases $(\epsilon_u)_i$ and $(\epsilon_w)_i$ are random uncorrelated numbers generated on a uniform distribution from $-\pi$ to π.

One of the drawbacks to the computation of the turbulence velocities by these summations is the intensive computational requirements. Trigonometric function computations are especially time-consuming, and it is clear that a number of such computations is needed for each time step. The typical dynamic simulation of aircraft motion requires a time increment in the neighborhood of 0.01-0.02 s. For an aircraft flying at a speed of 250 ft/s, this corresponds to a spatial increment of 2.5-5 ft. If the turbulence components are computed at the same rate, the time required to compute the random functions can become a significant portion of the total computation time, an especially serious problem if real-time simulation is required. Thus, it behooves one to search for ways to reduce the computation time required for the generation of the aforementioned functions.

The first technique proposed to reduce computation time also provides a criterion for determining the specific frequencies that divide the spectral densities into segments. If it is required that each segment contain the same fraction of the total power in the spectrum, then each sine function in the time series will have the same amplitude and can be factored out of the summation. Assuming this fraction to be denoted by f, we can compute the amplitudes from the equations

$$A_u = \sigma_u (2f)^{1/2} \tag{9}$$

$$A_w = \sigma_w (2f)^{1/2} \tag{10}$$

Thus the u and w functions can be written as

$$u(x) = A_u \sum \sin[(\Omega_u)_i x + (\epsilon_u)_i] \tag{11}$$

$$w(x) = A_w \sum \sin[(\Omega_w)_i x + (\epsilon_w)_i] \tag{12}$$

This methodology of dividing the spectrum into segments improves the computational efficiency by eliminating the need to multiply each sine function by a separate amplitude. It also equalizes the importance of each term in the series, since each term represents the same fraction of the total power in the spectrum. Thus, the computational efforts for generating each sine function are equally justified.

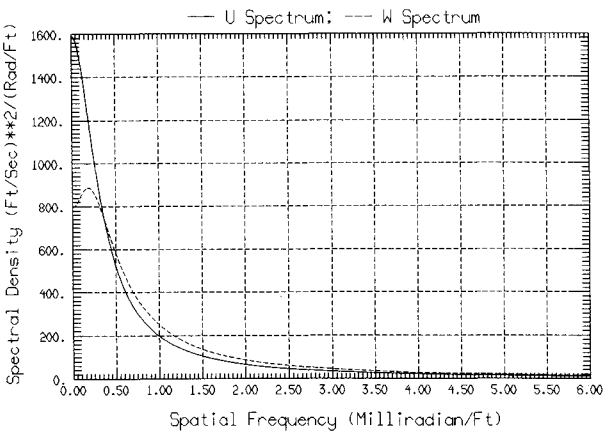

Fig. 1 Von Kármán spectra.

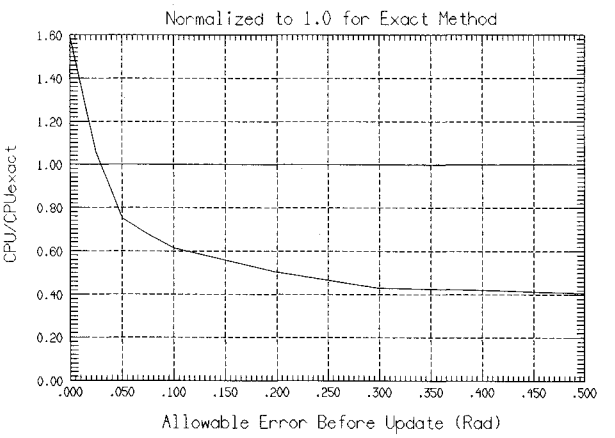

Fig. 2 CPU time comparison.

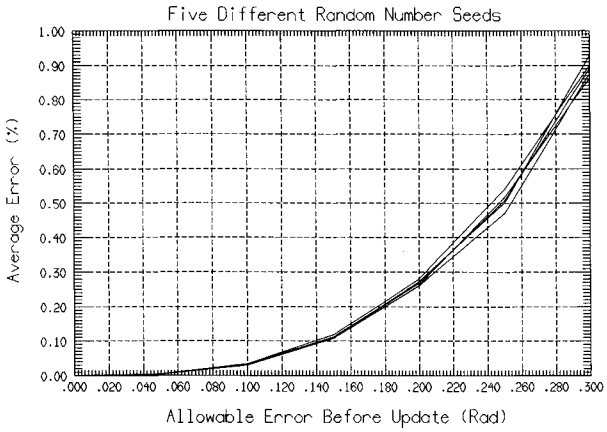

Fig. 3 Errors in u using approximate method.

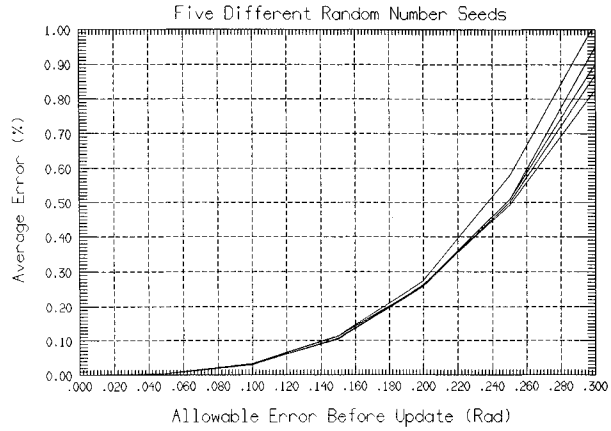

Fig. 4 Errors in w using approximate method.

For a given value of the nondimensional fraction f (e.g., $f = 1/100$), the functions u and w each can be characterized by a single amplitude plus a sequence of centroidal frequencies associated with the ensemble of fractional power segments. For the results presented in this paper, a value of $f = 0.01$ was chosen; that is, each fractional segment of the power spectra corresponded to 1% of the total power in the spectrum. Reference 5 suggests the use of 15 or more frequencies for an accurate approximation of ship motion, based on power spectra that are somewhat similar to the von Kármán turbulence spectra; however, the author of Ref. 3 used only six sinusoidal terms and found that the error was less than 5% "in most cases." The question of how many terms should be used in generating the random function is not a subject of this paper. Each analyst has his own concept of the accuracy that his problem requires and must make his choice accordingly. The selection of 100 sinusoidal terms for this investigation was purely arbitrary and in no way implies that such a number is required. However, using the time-saving methods presented in this paper, it can be stated that the use of as many as 100 terms does not appear to introduce computational difficulties.

The frequency boundaries for the segments corresponding to $f = 0.01$ were determined using a computer program to numerically integrate the area under the spectral density curve. Whenever the accumulated area was found to exceed an integral multiple of the selected power fraction, the value of the frequency associated with that multiple was determined by interpolation between the current and previous frequencies. Then the centroidal frequency for the segment was calculated using the trapezoidal formula. However, the last 1% segment for each curve was discarded, since the centroidal frequency for that segment is unbounded. This is easily shown by noting that, for very large values of $L_u\Omega$,

$$1 + (1.339L_u\Omega)^2 \simeq (1.339L_u\Omega)^2 \tag{13}$$

so the value of the centroidal frequency corresponding to the last 1% of the spectral power in the Φ_u spectrum can be approximated (if it exists) as follows:

$$(0.01)\bar{\Omega}_{100} = \int_{\Omega_i}^{\infty} \Omega\Phi_u \, d\Phi$$

$$\simeq \sigma_u^2 (2L_u/\pi) \int_{\Omega_i}^{\infty} \Omega(1.339L_u\Omega)^{-5/3} \, d\Omega \tag{14}$$

where Ω_i is the frequency separating the 99th from the 100th segments. Carrying out the indicated integration shows that the centroidal frequency of the 100th segment is unbounded. A similar analysis for the centroidal frequency of the 100th segment for the Φ_w spectrum would lead to the same conclusion. Thus, the last fractional segment of each spectrum was discarded and considered to be an acceptable error in the formulation.

An alternative approach would be to select an arbitrarily large frequency as an upper bound to the spectrum and subdivide the spectrum up to that frequency into the desired fractional segments. This would result in a slight shift in the frequency ensembles characterizing the functions u and w by an amount determined by the magnitude of the upper bound frequency selected. Also, the amplitudes A_u and A_w would be adjusted slightly by an amount that would depend on the magnitude of the upper bound frequency. A third "throw-away" policy would be to set a cutoff frequency to correspond to the point in the spectrum at which the spectral density reduces to a value equal to a specified percentage of the maximum density. The author of Ref. 4 used such a policy, with the cutoff frequency corresponding to a spectral density of 4% of the maximum.

Inspection of the von Kármán spectra shown in Fig. 1 shows that the greatest power lies in the low-frequency ranges. The nature of aircraft dynamics requires computation update frequencies of 50–100 times per second, which, for a typical light utility craft airspeed of 250 ft/s, correspond to variations in the space variable of an update every 2.5–5 ft of forward motion. For jet aircraft, a typical range of airspeeds would be from 500 to 1000 ft/s, for which simulation updates might be required every 10–20 ft (corresponding to an update frequency of 50 times per second). From this it is readily seen that the arguments of the majority of the sine functions in Eqs. (7) and (8) vary only slightly from one computation to the next. This suggests the practicality of using small-angle approximations to compute the sine functions until the variations from a reference value become large enough to require that the reference be updated. If we assume that the reference value for a particular sine function is x_{ref_i}, and δx_i is the variation from x_{ref_i}, then

$$\sin[\Omega_i(x_{\text{ref}_i} + \delta x_i) + \epsilon_i] = \sin(\Omega_i x_{\text{ref}_i} + \epsilon_i)\cos(\Omega_i \delta x_i)$$

$$+ \cos(\Omega_i x_{\text{ref}_i} + \epsilon_i)\sin(\Omega_i \delta x_i) \tag{15}$$

The following small-angle sine and cosine approximations are used:

$$\cos(\Omega_i \delta x_i) \simeq 1 - (\Omega_i \delta x_i)^2/2 \tag{16}$$

$$\sin(\Omega_i \delta x_i) \simeq \Omega_i \delta x_i \tag{17}$$

These small-angle approximations, when substituted into Eq. (15), then yield:

$$\sin[\Omega_i(x_{\text{ref}_i} + \delta x_i) + \epsilon_i] \simeq [1 - (\Omega_i \delta x_i)^2/2]\sin(\Omega_i x_{\text{ref}_i} + \epsilon_i)$$

$$+ (\Omega_i \delta x_i)\cos(\Omega_i x_{\text{ref}_i} + \epsilon_i) \tag{18}$$

This approximation may be simplified further by omitting the squared term in Eq. (16), in which case Eq. (18) is reduced to a linear variation about the reference value. This would simplify the computational algorithms but would require more frequent updating to maintain a given level of accuracy. Alternatively, a cubic term could be added to Eq. (17) to improve the accuracy of the sine approximation, thereby extending the time between updates of the reference values but increasing computational complexity. These variations were not considered in this paper; only the approximations given in Eqs. (16) and (17) were considered.

A computer program was written to compute random functions u and w for values of x from 0 to 50,000 ft in increments of 10 ft, using sine functions corresponding to 1% increments of the power spectral density. Thus, 99 terms were used in the computation of each function for each time step, since the last 1% of each spectral density function was discarded. The program was designed to generate the random functions using either of two options. If the first option was chosen, the functions would be calculated by recomputing the values of each sine term when the x variable was updated to a new value. This method will be referred to as the "exact" method. The second option, called the "approximate" method, uses Eq. (18) for the sine computations and requires an additional input from the user, a specification of the allowable deviation from a reference value before updating the reference. The program was written in Fortran 77 language and run on the VAX computers in the E-Systems Computation Center. A listing of this program, which reveals the methodology for updating the reference angle for each individual sine function, may be obtained by contacting the author.

The VAX performance and coverage analyzer (PCA) was used to measure CPU time for each option. A comparison of these CPU times for a range of allowable deviations before update is shown in Fig. 2, in which CPU time has been normalized to 1 for the exact method. It is seen from the curve that for very small values of update deviation, the approximate method required more CPU time than did the exact method. The reason for this is that the computation time required for testing each deviation from the reference and updating the reference, when required, with both a sine and a cosine computation was greater than the time saved by not having to compute the sine functions at each new time update. It is also seen from the figure that the break-even error is approximately 0.03 rad. Beyond this point, the reduction in CPU time continues rather sharply out to a deviation of approximately 0.1 rad, after which it begins to level off; for deviations greater than 0.3 rad, little further reduction occurs. At this point, the reduction in CPU time is approximately 57%.

The reduction achieved in computation time by use of the approximations described, however, must be traded against the loss of accuracy. To address this issue, a number of computer runs were made in which comparisons were made between a function computed from the exact equations and one computed using the approximations of Eq. (18). As in the CPU analysis, the spectral densities Φ_u and Φ_w were divided into 1% power segments and initial random phases generated for each sine function. The random functions were computed, as before, for values of x ranging from 0 to 50,000 ft in increments of 10 ft. Thus, a total of 5000 points were computed for each function. At each value of x, the function was calculated by each method and the results compared. These computations were repeated for different values of the allowable update deviation. A history of the errors at each point was recorded, and at the end of the function generation an average absolute error was computed and divided by the function standard deviation. This normalized error is shown in Fig. 3 for the u function and in Fig. 4 for the w function. It is noted that each figure shows several curves. Each curve represents functions that were generated using the same seed number for the random numbers generated, thus assuring that the same set of random phases would be used with each random function computed. The same set of seed numbers was used for the u function generation as for w. The variation from one curve to another is a measure of the repeatability of the results. It is seen that regardless of the seed number supplied, the results are reasonably consistent and predictable.

The information from Figs. 2–4 allows the analyst to determine the desired balance between computational speed and accuracy. For example, a choice of 0.1 rad allowable variation before updating introduces an error of approximately 0.032% in the random functions generated and reduces computation time in the neighborhood of 39%. Increasing the allowable variation before updates to 0.2 rad will increase the savings in computation time to approximately 50% but will result in an average error of approximately 0.266% in the random function generated. The analyst must decide the most desirable compromise between accuracy and computational speed. Also, remember that the results shown in Figs. 2–4 are based on a breakdown of the power spectra into segments, each of which is 1% of the total power. If a different breakdown of the power is desired, other tradeoff curves should be generated to provide a basis for the decision regarding the allowable variation between reference updates.

A typical pair of spatially referenced random functions were computed using the sum-of-sinusoids method, based on the breakdown of the Φ_u and Φ_w spectra. These functions are shown in Fig. 5 and were computed using the exact method of computation of the sine functions. A listing of the computer program used to compute these functions may be obtained by contacting the author.

Dryden Turbulence

The Dryden form of the spectral densities Φ_u and Φ_w, defined analytically in Eqs. (4–6), is shown in graphical form in

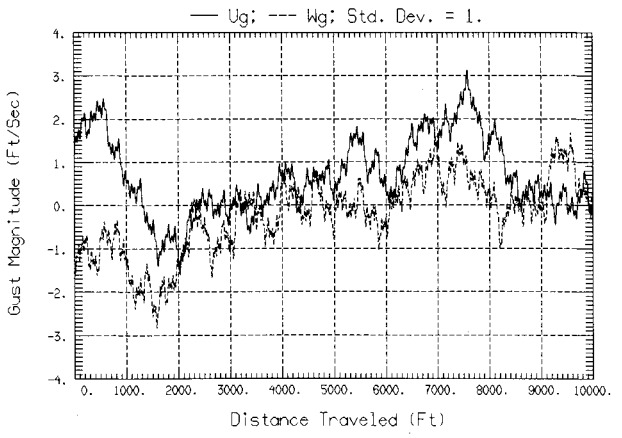

Fig. 5 Sample u_g and w_g histories.

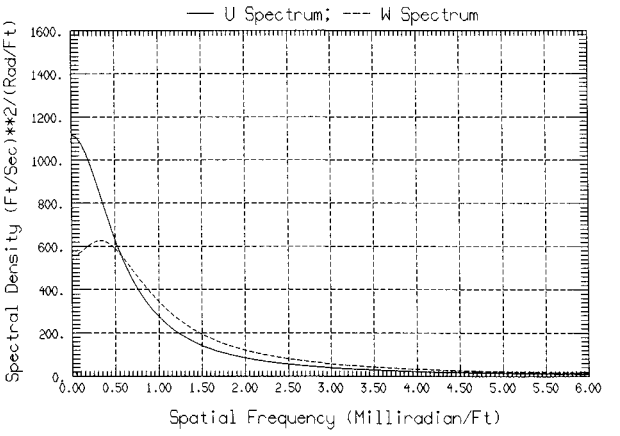

Fig. 6 Dryden spectra.

Fig. 6 over a limited frequency range. As in the case of the von Kármán spectra, the function Φ_v is identical in form to Φ_w and has been omitted. The curves shown correspond to scale lengths of 1750 ft, as recommended in Ref. 1, and unity values of σ_u and σ_w. To reflect higher levels of turbulence, the curves would be multiplied by the desired values of σ_u^2 and σ_w^2.

The simulation of atmospheric turbulence having statistical characteristics corresponding to the Dryden spectra presents the analyst with more options than in the case where the von Kármán spectra are to be used. The sum-of-sinusoids method proposed for use with the von Kármán spectra could be used equally well with the Dryden spectra. However, unlike the von Kármán spectra, the random functions associated with the Dryden spectra can be readily generated by passing white noise (or, more practically, band-limited white noise) through appropriate linear filters. We will discuss only this latter approach in this paper. The analyst can make his own determination of which method best suits his purpose.

It is well known[7] that white noise having a spectral density Φ_{wn}, when passed through a filter having a Laplacian transfer function $F(s)$, will produce a random function having a spectral density of

$$\Phi_f(\Omega) = \Phi_{wn} \mid F(j\Omega) \mid^2 \tag{19}$$

From the definition of the Dryden spectra in Eqs. (4–6), it can be shown that the desired filters for generating u and w random turbulence velocities in this way are

$$F_u(s) = \frac{1}{1 + L_u s} \tag{20}$$

$$F_w(s) = \frac{1 + (3)^{1/2} L_w s}{(1 + L_w s)^2} \tag{21}$$

Remember that x was chosen as the independent variable in this study; therefore, the Laplacian operator s in these transfer functions corresponds to differentiation with respect to the spatial variable x. Transformation to the time domain is effected through the equation $x = V \cdot t$. Likewise, in the following derivations, integration steps Dx are related to time increments Dt through the equation Dx = $V \cdot$ Dt.

As in the case of von Kármán turbulence, the consideration of the v component is omitted because of its functional equivalence to the w component. It also can be generated by passing white noise from an independent source through the same type of filter as that used to generate the w function.

The inputs to these filters are obtained from random function generators that output a discrete sequence of uncorrelated numbers having a Gaussian distribution. The function so generated can be considered to be an analog function, with correlation induced by the finite sampling time. This is a somewhat

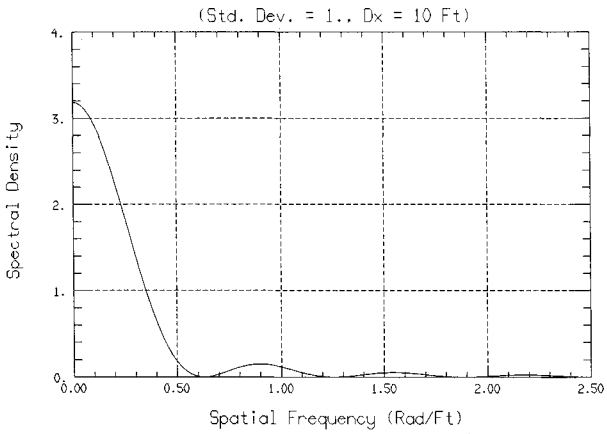

Fig. 7 Spectral density of random input.

unconventional approach that, it is hoped, will provide some insight into the physical process without undue involvement of esoteric mathematical techniques. The approach described has been used frequently by the author, and statistical analysis of the random functions generated in the manner described verify that the desired statistical characteristics are accurately reproduced.

Numbers are generated every Dx ft, each new number being uncorrelated with all previous numbers. The function so generated can be considered as an analog function in which each sampled value is constant through Dx ft, after which a new value will be sampled. Defining the correlation function for the generic variable $y(x)$ as $R(\xi) = E\{y(x) \cdot y(x + \xi)\}$ (where E is the expectation operator), we can show that, for the function generated,

$$R(\xi) = \sigma_{wn}^2 (1 - \xi/\mathrm{D}x) \qquad \text{for} \qquad \xi < \mathrm{D}x \tag{22}$$

and

$$R(\xi) = 0 \qquad \text{for} \qquad \xi \geq \mathrm{D}x \tag{23}$$

where σ_{wn} is the standard deviation of the Gaussian random function.

Since the spectral density of a random function is the Fourier transform of its correlation function, the following relationship holds:

$$\Phi(\Omega) = (2/\pi) \int_0^\infty R(\xi) \cos(\Omega\xi)\, \mathrm{d}\xi \tag{24}$$

Performing the indicated integration of the correlation function described in Eqs. (22) and (23) produces a spectral density function given by

$$\Phi(\Omega) = (2\sigma_{wn}^2 / \pi \Omega^2\, \mathrm{D}x)[1 - \cos(\Omega\, \mathrm{D}x)] \tag{25}$$

The spectral density defined by Eq. (25) is shown for a value of Dx = 10 ft in Fig. 7 for $\sigma_{wn} = 1$. The largest value of Ω shown in this figure is 2.5; however, this is a much larger frequency than our range of interest, as will be shown in the next paragraph.

For sufficiently small values of Ω Dx, Eq. (25) can be approximated by

$$\Phi(\Omega) = \sigma_{wn}^2\, \mathrm{D}x/\pi \tag{26}$$

Thus, the spectral density of the sample-hold random function can be considered constant out to a frequency at which the small-angle approximation is no longer valid. Such a frequency, however, is quite large in comparison to the frequencies of interest. For example, if we assume Dx = 10 ft, a typical integration step size for an aircraft simulation, a frequency of Ω = 0.05 rad/ft represents only about a 2% lower value than that obtained from the approximation of Eq. (26). At this frequency, the Φ_u spectrum is reduced by a factor of approximately 1.3×10^{-4} and the Φ_w spectrum by 3.9×10^{-4} in comparison to their zero frequency values. Thus, it can be concluded that the random function will have an essentially constant density given by Eq. (26) over the range of frequencies of interest.

If the spectral density of the random function can be considered to be constant as defined by Eq. (26), then the spectral densities of the filtered signals are

$$\Phi_u(\Omega) = (\sigma_{wn}^2\, \mathrm{D}x/\pi) \frac{1}{1 + (L_u\Omega)^2} \tag{27}$$

$$\Phi_w(\Omega) = (\sigma_{wn}^2\, \mathrm{D}x/\pi) \frac{1 + 3(L_w\Omega)^2}{[1 + (L_w\Omega)^2]^2} \tag{28}$$

For the spectral densities of the filtered signals to correspond to those of the Dryden spectra, it is seen by inspection that the standard deviations of the unfiltered signals must be as follows.

u-velocity filter:

$$\sigma_{wn} = \sigma_u (2L_u/\mathrm{D}x)^{1/2} \tag{29}$$

w-velocity filter:

$$\sigma_{wn} = \sigma_w (L_w/\mathrm{D}x)^{1/2} \tag{30}$$

After generating uncorrelated random functions x_u and x_w with standard deviations given by Eqs. (29) and (30), it remains to filter these functions through $F_u(s)$ and $F_w(s)$ to obtain random functions having the desired characteristics. For the u function, the filter differential equation to be solved is

$$L_u u' + u = x_u \tag{31}$$

where the prime denotes differentiation with respect to x. A difference equation is obtained by approximating u', u, and x_u at the midpoint of the interval between x_{i-1} and x_i. Thus,

$$u' \simeq (u_i - u_{i-1})/\mathrm{D}x \tag{32}$$

$$u \simeq (u_i + u_{i-1})/2 \tag{33}$$

$$x_u = (x_u)_i \tag{34}$$

Substituting Eqs. (32-34) into (31) and solving for u_i leads to

$$u_i = A_u u_{i-1} + 2B_u (x_u)_{i-1} \tag{35}$$

where

$$R_u = \frac{\mathrm{D}x}{2L_u}, \qquad A_u = \frac{1 - R_u}{1 + R_u}, \qquad B_u = \frac{R_u}{1 + R_u}$$

The generation of the w function is presented as a two-step process, representing first a filtering through a first-order lag, followed by a lead-lag filtration. The intermediate function between these two steps is defined by the variable y. This approach leads to two differential equations that must be satisfied:

$$L_w y' + y = x_w \tag{36}$$

$$L_w w' + w = (3)^{1/2} L_w y' + y \tag{37}$$

Making approximations to y', y, x_w, w', w, and y at the midpoint of the interval between x_i and x_{i-1}, as before, leads to the following recursive formulas for y_i and w_i:

$$y_i = A_w y_{i-1} + 2B_w (x_w)_{i-1} \tag{38}$$

$$w_i = A_w w_{i-1} + B_w (y_i + y_{i-1}) + C_w (y_i - y_{i-1}) \tag{39}$$

where

$$R_w = \frac{\mathrm{D}x}{2L_w}, \quad A_w = \frac{1 - R_w}{1 + R_w}, \quad B_w = \frac{R_w}{1 + R_w}, \quad C_w = \frac{(3)^{1/2}}{1 + R_w}$$

It is noted that the relations between the standard deviations of the filtered and unfiltered signals, as given in Eqs. (29) and (30), could have been obtained equally well from a variance analysis of the digital filtering algorithms defined in Eqs. (35), (38), and (39).

Angular Velocity Disturbance

To this point, consideration has been limited to turbulence associated with translational components of velocity. Use of these components alone is equivalent to the assumption of uniform immersion of the aircraft in the gust; that is, the simulated turbulence is assumed to act uniformly over the dimensions of the aircraft. More accurate estimates of the effects of the turbulence can be realized by considering the variations of the velocities over the dimensions of the aircraft. Yaw and pitch effects can be evaluated numerically based on spatial variations of the v and w components of turbulence. Roll effects, however, must be obtained by passing an uncorrelated random function through a shaping filter to produce a random function having the desired variance and spectral characteristics. The spectral density of the roll function, defined in Ref. 1, is

$$\Phi_p(\Omega) = \frac{\sigma_w^2}{L_w} \frac{0.8(\pi L_w/4b)^{1/3}}{1 + (4b\Omega/\pi)^2} \tag{40}$$

where b is the wingspan of the aircraft. Using an approach similar to that used for u and w, we can show that a function with the desired characteristics can be obtained by first generating a random uncorrelated series of numbers with a Gaussian distribution and filtering through a Laplacian transfer function given by

$$F_p(s) = \frac{1}{1 + L_p s} \tag{41}$$

where the Laplacian is defined, as before, relative to the spatial variable x and

$$L_p = 4b/\pi \tag{42}$$

To produce a filtered function having the correct magnitude, it can be shown by the same method used previously that the standard deviation of the unfiltered signal must be

$$\sigma_{wn} = \sigma_w [(0.8\pi/L_w\ \mathrm{D}x)(\pi L_w/4b)^{1/3}]^{1/2} \tag{43}$$

The filtering algorithms required to generate the required random function for simulating roll disturbances are similar to those used in the u function calculation:

$$p_i = A_p p_{i-1} + 2B_p (x_p)_{i-1} \tag{44}$$

where

$$A_p = \frac{1 - R_p}{1 + R_p}, \qquad B_p = \frac{R_p}{1 + R_p}, \qquad R_p = \frac{m\ \mathrm{D}x}{8b}$$

It is recommended that the analyst, after implementing the derived algorithms, verify that the magnitudes of the turbulence amplitudes are correct by setting up accumulators in his simulation that sum the squares of the amplitudes, then perform the computations

$$\hat{\sigma}_w = \left(\sum_{i=1}^{N} (w_i^2/N) \right)^{1/2}$$

For a sufficiently large N, the estimates of the standard deviations computed in this manner should approach the specified values.

Application of the Disturbances to Aircraft Dynamics

The equations of motion of an aircraft are universally expressed in body coordinates, in which U, V, and W represent velocity components of the aircraft center of gravity along the x, y, and z axes of the aircraft, respectively, and P, and Q, and

R represent the angular velocities relative to these same axes. The aerodynamic forces and moments on the aircraft are computed using aerodynamic coefficients and derivatives, as appropriate. The turbulence effects are incorporated by combining the random functions with the appropriate elements of the dynamic state vector for the purpose of determining aerodynamic effects. Thus, $U_A = U + u$, $V_A = V + v$, $W_A = W + w$, $P_A = P + p$, $Q_A = Q + q$, and $R_A = R + r$. Wherever these terms are used in evaluating the aerodynamic forces and moments, incorporation of the turbulence terms as shown ensures that the turbulence effects will be properly modeled.

Although Ref. 1 defines spectral density functions for the yawing and pitching turbulence (r and q) as well as for the roll turbulence (p), it points out that the yawing effect is correlated with the lateral turbulence velocity and the pitching turbulence is correlated with the vertical turbulence velocity. The simplest way to reflect this correlation is to use the functions v and w to estimate effective values of r (yawing angular velocity) and q (pitching angular velocity) based on numerical variations along the longitudinal axis of the aircraft. Since the primary contributor to aerodynamic pitching effects is the horizontal tail and the primary contributor to aerodynamic yawing effects is the vertical tail, it is recommended that the equivalent yaw turbulence angular velocity be computed from

$$r = (v_i - v_{i-n})/d_v \tag{45}$$

where v_i is the current value of the function v, and v_{i-n} is the past value that most closely coincides with the location of the vertical tail at the current time. This is easily visualized if one imagines the aircraft progressing through the turbulence field a step at a time. The turbulence components just computed are assumed to act at the center of gravity of the aircraft, and past values progress to the rear of the aircraft in steps of length Dx. The value of d_v, then, would be n Dx.

The equivalent pitch turbulence angular velocity q is computed in a similar manner from the w function, that is,

$$q = (w_i - w_{i-m})/d_w \tag{46}$$

where w_i is the current value of the function w, and w_{i-m} is the past value that most closely coincides with the location of the horizontal tail at the current time. The value of d_w is m Dx. Usually, the horizontal tail will be located very near the vertical tail, so that n and m will be very nearly the same, if not exactly the same, from which it would follow that d_v and d_w would be almost, if not exactly, equal. The exception to this case would be the case of a canard for pitch control. In this case, the current value of the w function should represent a vertical disturbance amplitude at the canard, and a value computed m points in the past should be used with it, as in Eq. (46), to evaluate the effective pitch disturbance. In this case, the past value w_{i-m} should be used as the vertical disturbance acting at the aircraft center of gravity.

In setting up the algorithms to save and use past values of the functions v and w to calculate effective yaw and pitch disturbances, a typical technique is to construct an array of values representing sequential past values of the function and use these as needed. At the end of each computation step, the values in the array are then shifted by one (either up or down, depending on the analyst's choice), letting one of the values fall out the end and replacing the other end point by the newest value of the function. A better method uses a pointer that shifts one point at each new time point. The value at the pointer is replaced at each computation step by the newest value. The pointer continues to shift by one unit at each step until it reaches the end of the array, after which the pointer position is transferred to the other end of the stack. This technique is especially time conservative if the stack is a very long one.

Concluding Remarks

Methods have been shown for digital implementation of the von Kármán and Dryden turbulence models defined in MIL-F-8785C. For the von Kármán model, modifications to the standard sum-of-sinusoids method have been evaluated to determine the resulting improvements in computational efficiency. A potential savings of approximately 60% in computation time was identified, at the expense of a reduction of accuracy. For the Dryden model, digital filtering algorithms were presented, and the amplitude of the unfiltered signal required to obtain the desired filtered amplitude was addressed. Rotational velocity effects were also addressed, and a method was suggested for incorporating them into a dynamic simulation. Application of random turbulence to an aircraft simulation was discussed.

References

[1]"Flying Qualities of Piloted Airplanes," MIL-F-8785C, Nov. 5, 1980.

[2]St. Denis, M., and Pierson, W. J., "On the Motions of Ships in Confused Seas," *Transactions of the Society of Naval Architects and Marine Engineers,* Vol. 61, 1953, pp. 280–357.

[3]Fortenbaugh, R. L., "Progress in Mathematical Modeling of the Aircraft Operational Environment of DD963 Class Ships," AIAA Atmospheric Flight Mechanics Conference (Boulder, CO), Aug. 6–8, 1979 (AIAA Paper 79–1677).

[4]Fortenbaugh, R. L., "Mathematical Models of the Aircraft Operational Environment of DD963 Class Ships," Vought Corporation, Vought Rept. 2-55800/8R-3500, Dallas, TX, Sept. 26, 1978.

[5]Brown, R. G., and Camaratta, F. A., NAVAIRENGCEN Ship Motion Computer Program, Naval Air Engineering Center Rept. MISC-903-8, Lakehurst, NJ, 1978.

[6]Beal, T. R., "Feasibility Study of Shipboard Recovery of the Aquila Remotely Piloted Vehicle," TRB-2, Oct. 31, 1985 (published by the author).

[7]Davenport, W. B., and Root, W. L., *An Introduction to the Theory of Random Signals and Noise,* McGraw-Hill, New York, 1958.